

## Structural and thermoelectric properties of the $\text{Pr}_2\text{Zr}_2\text{O}_7$ compound

### Propiedades estructurales y termoeléctricas del compuesto $\text{Pr}_2\text{Zr}_2\text{O}_7$

QUIROZ-RODRÍGUEZ, Adolfo<sup>1†\*</sup>, GUARNEROS-AGUILAR, Cesia<sup>2</sup> and AGUSTIN-SERRANO, Ricardo<sup>3</sup>

<sup>1</sup>Universidad Tecnológica de Xicotepec de Juárez, Industrial and Petroleum Maintenance Area. Av. Universidad Tecnológica No. 1000, Col. Tierra Negra, Cd. Xicotepec de Juárez, Pue., México. C.P. 73080

<sup>2</sup>CONACYT- Instituto Politécnico Nacional, Materials and Technologies for Energy Health and Environment (GESMAT), CICATA Altamira, Km 14.5 Street Tampico-Puerto Industrial Altamira, Altamira, Tamaulipas, México. C. P. 89600

<sup>3</sup>Benemérita Universidad Autónoma de Puebla. Faculty of Mathematical Physical Sciences, Av. San Claudio y 18 Sur, Ciudad Universitaria, Puebla, Pue. México. C. P. 72570

ID 1<sup>st</sup> Author: Adolfo, Quiroz-Rodríguez / ORC ID: 0000-0002-9685-9455, arXiv Author ID: adolfo-79, CVU CONACYT ID: 105471

ID 1<sup>st</sup> Coauthor: Cesia, Guarneros-Aguilar / ORC ID: 0000-0001-8751-4394, CVU CONACYT ID: 46832

ID 2<sup>nd</sup> Coauthor: Ricardo, Agustin-Serrano / ORC ID: 0000-0002-6468-7548, CVU CONACYT ID: 165478

DOI: 10.35429/EJDRC.2019.9.5.4.9

Received July 28, 2019; Accepted September 25, 2019

#### Abstract

In this research, it is presented a detailed study of the structural and thermoelectric properties of the pyrochlore zirconium  $\text{Pr}_2\text{Zr}_2\text{O}_7$  compound prepared by solid-state reaction (SSR) in air at ambient pressure. The synthesized sample was characterized using powder X-ray diffraction. The thermal stability of the thermoelectric compound (TE)  $\text{Pr}_2\text{Zr}_2\text{O}_7$  was tested by thermogravimetric analysis (TGA) and differential thermal analysis (DTA). Scanning electron microscopy shows that the crystal size varies between 0.69 and 2.81  $\mu\text{m}$ . Electrical conductivity ( $\sigma$ ) of the sample calcined at 1400 °C presented values increase irregularly with the increasing temperature from 0.001 to 0.018  $\text{S cm}^{-1}$  as expected in a semiconductor material. The thermal conductivity is lower than 0.44 - 775  $\text{W m}^{-1} \text{K}^{-1}$  which is quite anomalous in comparison with the thermal conductivity of other oxides.

**Solid-state reaction, Pyrochlore compounds, Crystal structure**

#### Resumen

En esta investigación, se presenta un estudio detallado de las propiedades estructurales y termoeléctricas del compuesto pirocloro de circonio  $\text{Pr}_2\text{Zr}_2\text{O}_7$  preparado por reacción en estado sólido (SSR) en aire a presión ambiente. La muestra sintetizada se caracterizó utilizando difracción de rayos-X en polvo. La estabilidad térmica del compuesto termoeléctrico (TE)  $\text{Pr}_2\text{Zr}_2\text{O}_7$  se probaron mediante análisis termogravimétrico (TGA) y análisis térmico diferencial (DTA). Microscopía electrónica de barrido muestra que el tamaño del cristal varía entre 0.69 y 2.81  $\mu\text{m}$ . La conductividad eléctrica ( $\sigma$ ) de la muestra calcinada a 1400 °C presentó valores que aumentan irregularmente con el aumento de la temperatura de 0.001 a 0.018  $\text{Scm}^{-1}$  como se esperaba en un material semiconductor. La conductividad térmica es inferior a 0.44 - 775  $\text{W m}^{-1} \text{K}^{-1}$ , lo cual es bastante anómalo en comparación con la conductividad térmica de otros óxidos.

**Reacción en estado sólido, Compuestos de pirocloro, Estructura cristalina**

**Citation:** QUIROZ-RODRÍGUEZ, Adolfo, GUARNEROS-AGUILAR, Cesia and AGUSTIN-SERRANO, Ricardo. Structural and thermoelectric properties of the  $\text{Pr}_2\text{Zr}_2\text{O}_7$  compound. ECORFAN Journal-Democratic Republic of Congo. 2019, 5-9: 4-9

\* Correspondence to Author (email: adolfo.quiroz@utxicotepec.edu.mx)

† Researcher contributing first author.

## Introduction

Thermoelectric devices are a technology that converts waste heat into electric power or vice versa through the thermoelectric phenomena in semiconductor solids [1]. Since this technology is a direct energy conversion in solids, it has attracted a renewed interest as a fundamental technology for environmentally friendly energy conversion. In particular, thermoelectric power generation has been now considered as a possible renewable energy source. The thermoelectric materials comprises from semimetals, semiconductors, ceramics to polymers. However, thermoelectric oxide materials have been extensively investigated as a promising thermoelectric power generator because they are stable at high temperatures in air. Oxides were considered to be poor thermoelectric materials, but after the discovery of a large thermoelectric power factor in  $\text{Na}_x\text{CoO}_2$ , some cobalt oxides are recognized as good p-type thermoelectric oxides [2,3]. In contrast, not yet discovered is an n-type counterpart to the cobalt oxides. Some of the transparent conductors such as ZnO and  $\text{In}_2\text{O}_3$  show indeed good thermoelectric performance above 1000 K, [4,5] but the lattice thermal conductivity is much higher than the conventional thermoelectric materials. The doped titanates [6,7] and niobates [8-10] are fairly good n-type thermoelectric materials at room temperature, but they are easily oxidized at high temperature to lose conductivity in air. Recently, a large Seebeck coefficient and low thermal conductivity have been reported in polycrystalline samples of the double perovskite ruthenate  $\text{Sr}_2\text{LRuO}_6$  (L; rare-earth) [11]. Although the magnetic properties and ground states of the titanate pyrochlores have been investigated in detail, similar studies of the zirconate pyrochlores have been hampered by the lack of large, good quality single crystals. With the exception of a few investigations on  $\text{Pr}_2\text{Zr}_2\text{O}_7$  single crystals [12-14], most of the research on the zirconate pyrochlores has used powder samples [15-22].

The aim of this investigation was to synthesize the polycrystalline  $\text{Pr}_2\text{Zr}_2\text{O}_7$  compound via the solid-state reaction method and a detailed study of the precise time for obtaining the compound. In the present contribution, we report the relationship between structural, Seebeck Coefficient, electrical conductivity and thermal conductivity properties of the pyrochlore  $\text{Pr}_2\text{Zr}_2\text{O}_7$ .

These properties make rare-earth zirconates suitable for a variety of applications such as solid electrolytes, catalysts, nuclear waste forms, and especially high-temperature TBCs (Thermal barrier coatings) materials [23].

## Materials and Methods

Polycrystalline sample of the  $\text{Pr}_2\text{Zr}_2\text{O}_7$  compound was synthesized by solid-state reaction at ambient pressure in air. The starting materials were  $\text{ZrO}_2$  (Riedel-de Haën pure), and  $\text{Pr}_2\text{O}_3$  (Cerac, 99.9 %). Structure and purity of the materials were determined by XDR. The stoichiometric mixture of the starting materials was done in air during 30 minutes, agitated with an agata mortar, resulting in homogenous slurry [24].

The resultant  $\text{Pr}_2\text{Zr}_2\text{O}_7$  mixture was compressed into pellets (13 mm diameter,  $1.0-1.5 \pm 0.05$  mm thickness) by applying a pressure of 3 tons/cm<sup>2</sup> during 5 minutes under vacuum. The resulting compacted specimens were then sintered in air at 1400 °C during 3 days and then cooled down to room temperature following the natural cooling of furnace to 7 h.

The thermal behavior of  $\text{Pr}_2\text{Zr}_2\text{O}_7$  compound was studied from 25 to 1200 °C through differential thermal analysis (DTA), and thermogravimetric analysis (TGA) using measuring equipment SDT Q600, TA Instruments. Sample was characterized by X-ray powder diffraction (XRD) using an APD 2000 diffractometer with Cu K $\alpha$  radiation ( $\lambda = 1.5406 \text{ \AA}$ ) and a graphite monochromator.

Diffraction patterns were collected at room temperature in air, over the  $2\theta$  range  $10^\circ - 90^\circ$  with a step size of  $0.025^\circ$  and a time per step of 15 seconds. Changes in morphology and grain size were induced in the sample by performing different heat treatments during all the process of the sample preparation and examined by scanning electron microscopy (SEM) on a Hitachi S-3400N-II System.

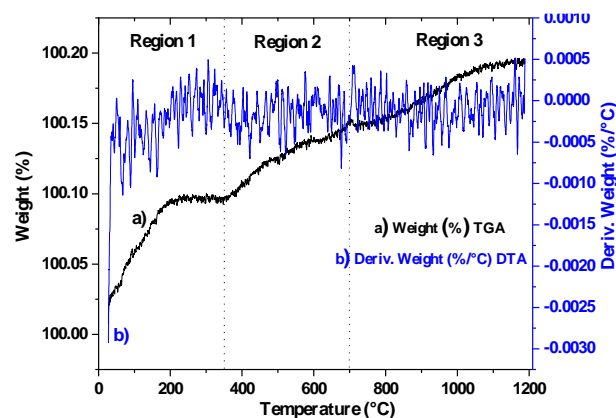
The 10.00 K.X micrograph was taken with a voltage of 20 kV, a current intensity of 1000 pA and WD = 10 mm. Energy Dispersive X-Ray (EDX) was performed on the same SEM system, which is equipped with an EDAX 9900 device.

For thermoelectric characterization, square-shaped compact of dimension 10 mm x 10 mm x 0.5 mm was prepared using a 3-ton hydraulic press, Seebeck coefficient and electric conductivity were measured simultaneously under a 10 sscm N<sub>2</sub> flux, from 100 to 800 °C in a high-precision SBA 458 Nemesis Netzsch system imposing a 0.05 A current; the heater voltage for Seebeck measurements was 1.0 V, the temperature increment was 5 Ks<sup>-1</sup>, and the temperature difference threshold is 15 K. The thermal conductivity was measured in a LFA 467 HyperFlash Netzsch apparatus equipped with a xenon flash lamp and an InSb detector, in the temperature range from 100 to 600 °C, with pulsed energy up to 10 J/pulse and pulse width of 20–1200 μs.

## Results and Discussions

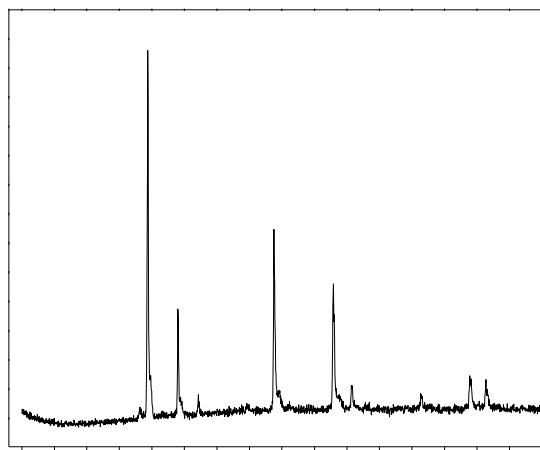
**Thermogravimetric Analysis (TGA).** The TGA curves are important to determine the temperatures to which the formation of organic matter and subproducts take place during the solid-state reaction method. The results obtained from this technique did help to control the process parameters to produce the Pr<sub>2</sub>Zr<sub>2</sub>O<sub>7</sub> compound. The TGA results obtained from the Pr<sub>2</sub>Zr<sub>2</sub>O<sub>7</sub> were analyzed separately and are shown in Figure 1. The TGA (a) curve is divided in three most relevant regions: 25–350 °C, 350–700 °C, and 700–1200 °C. In the next ascend TGA curve start with a hydrated material at room temperature up to 350 °C. After 350 °C an increase in curve means, the formation of Pr<sub>2</sub>Zr<sub>2</sub>O<sub>7</sub> compound (seen in some reaction conditions by XRD). Around 700 °C it is detected a weak lost of energy peak that may be due to the melting of reagents, binary and ternary compounds corroborated by XRD.

The DTA (b) curve for Pr<sub>2</sub>Zr<sub>2</sub>O<sub>7</sub> compound is presented in Figure 1. The sample present a first exothermic effect around 300 °C, which is unusual; it means that the structure that is obtained between 300 and 1200 °C is metaestable and the DTA exotherm signs a decrease in enthalpy of the sample and therefore a change to a more stable structure. For temperatures higher than 1200 °C, exothermic effects are observed that are important to understand the stability in the solid solution formation mechanism as its thermal stability.



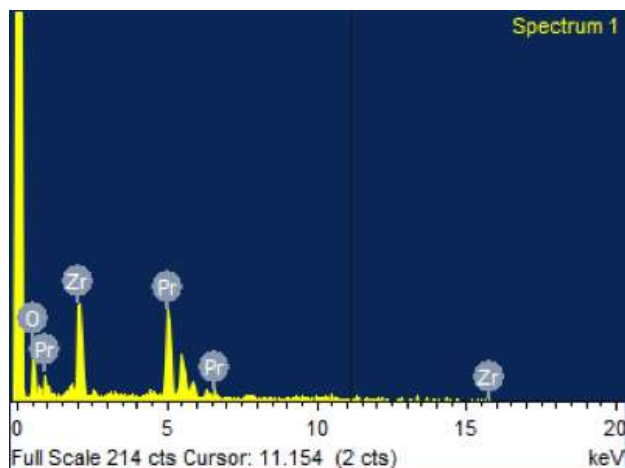
**Figure 1** TGA and DTA of the Pr<sub>2</sub>Zr<sub>2</sub>O<sub>7</sub> sample

Figure 2 presents the X-ray diffraction pattern of the sintered Pr<sub>2</sub>Zr<sub>2</sub>O<sub>7</sub> compound. The combination of the XRD and TGA analysis proved to be useful when observing the number of phases that changed during the applied heat treatments to Pr<sub>2</sub>Zr<sub>2</sub>O<sub>7</sub> sample. The solid line corresponds to a cubic polycrystalline phase with Fd $\bar{3}$ m (No. 227) space group and it is identified as Pr<sub>2</sub>Zr<sub>2</sub>O<sub>7</sub> compound with PDF (04-008-6354).



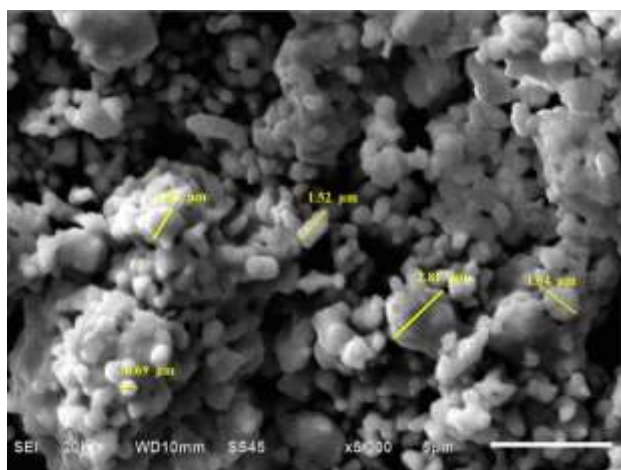
**Figure 2** XRD Pattern evolution of pyrochlore Pr<sub>2</sub>Zr<sub>2</sub>O<sub>7</sub> compound

The EDX elemental analysis of the Pr<sub>2</sub>Zr<sub>2</sub>O<sub>7</sub> compound is shown in Figure 3. The atomic percentage for the Pr, Zr and O was 54.14%, 28.11% and 19.75%, respectively.



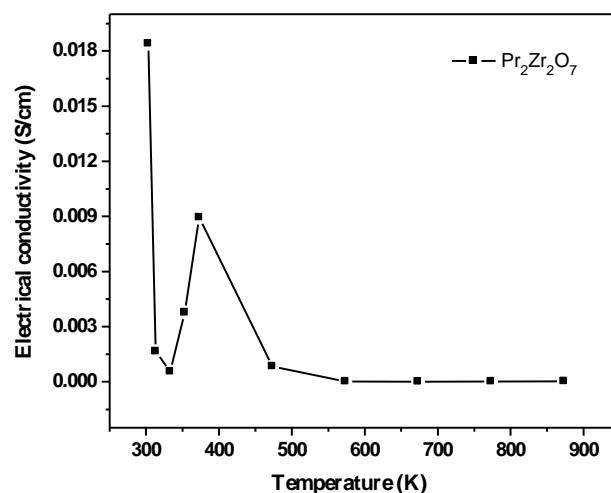
**Figure 3** Spectrum of EDX analysis for the  $\text{Pr}_2\text{Zr}_2\text{O}_7$  compound after applying the heat treatment at  $1400\text{ }^\circ\text{C}$  during 3 days

Figure 4 shows the elemental SEM mapping performed to the produced  $\text{Pr}_2\text{Zr}_2\text{O}_7$  compound. This analysis confirmed the homogeneous distributions of the  $\text{Pr}_2\text{Zr}_2\text{O}_7$  compound in the sample. The sample calcined at  $1400\text{ }^\circ\text{C}$  shows the formation of different particle sizes between  $0.69$  and  $2.81\text{ }\mu\text{m}$ , and some of them present a well-defined grain boundary, while the rest are agglomerations.



**Figure 4** SEM for the  $\text{Pr}_2\text{Zr}_2\text{O}_7$  compound

Electrical conductivity ( $\sigma$ ) of the sample calcined at  $1400\text{ }^\circ\text{C}$  is presented in Figure 5. Sample calcined at  $1400\text{ }^\circ\text{C}$  show a electrical conductivity low. The  $\sigma$  values increase irregularly with the increasing temperature from  $0.001$  to  $0.018\text{ Scm}^{-1}$  as expected in a semiconductor material [25].



**Figure 5** Temperature dependence of electrical conductivity for  $\text{Pr}_2\text{Zr}_2\text{O}_7$  sample obtained at  $1400\text{ }^\circ\text{C}$

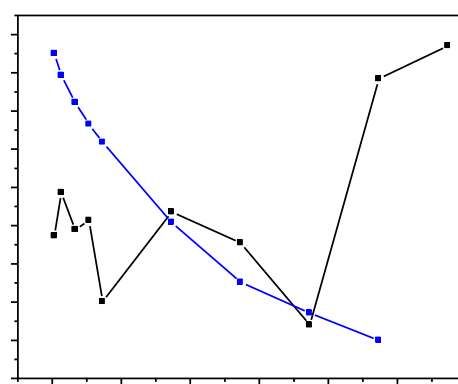


**Figure 6** Seebeck coefficient and thermal conductivity in the temperature range  $300\text{--}900\text{ }^\circ\text{K}$

Seebeck coefficient and thermal conductivity measured as a function of temperature are presented in Figure 6. The Fig. 6 (a) show  $S$  values, ranging from  $-0.00025$  to  $0.0005\text{ }\mu\text{VK}^{-1}$ , are positive and negative over the temperature range confirming the semiconductor p and n-character, where the holes and electrons are the main charge carriers. The p-character in  $\text{Pr}_2\text{Zr}_2\text{O}_7$  has been attributed to the deviation from stoichiometric composition and ionized and / or interstitial oxygens generate positive holes [26-28].

The sign for the sample is negative, and the magnitude systematically decreases with increasing temperature. These results show that the  $\text{Pr}^{+3}$  ion acts as a donor to supply electrons to the system. The calculated thermal conductivity of  $\text{Pr}_2\text{Zr}_2\text{O}_7$  ceramic as a function of temperature are plotted in Fig. 6 (b). The thermal conductivity of  $\text{Pr}_2\text{Zr}_2\text{O}_7$  ceramic gradually decrease with the increase of temperature up to  $800\text{ }^\circ\text{C}$ , which is attributed to the lattice thermal conduction.

## Acknowledgments

The authors acknowledge the financial support provided by Universidad Tecnológica de Xicotepec de Juárez and Karla Eriseth Reyes Morales from Instituto de Investigaciones en Materiales of Universidad Nacional Autónoma de México, for performing thermogravimetric analysis (TGA) measurements. SBA 458 Nemesis and LFA 467 HyperFlash Netzsch systems were acquired by Project 252705 from CONACYT INFR-2015-01. The authors acknowledge to MTA Juan Jesús Reyes for Seebeck coefficient and thermal conductivity measurements.

## Conclusion

In this work, was obtained polycrystalline  $\text{Pr}_2\text{Zr}_2\text{O}_7$  compound by solid-state reaction method in air at atmospheric pressure. SEM micrograph shows the effect of heat treatments and processing route on the grain morphology of the compound. The  $\sigma$  values increase irregularly with the increasing temperature from 0.001 to 0.018  $\text{Scm}^{-1}$  as expected in a semiconductor material.

## Perspectives

As future considerations, with the result of the measurements obtained in this study we have as future research to improve the electrical conductivity property of our new compounds using small quantities of  $\text{Sr}^{+2}$  doping and to decrease the thermal conductivity, which will help us obtain a zirconium pyrochloro with better thermoelectric properties for applications in solid electrolytes, catalysts, nuclear waste forms, and especially high-temperature TBC materials.

## References

- [1] Mahan, G. (1997). Good thermoelectrics. *Solid state physics*, 51, 81-157.
- [2] Terasaki, I., Sasago, Y., and Uchinokura, K. (1997). Large thermoelectric power in  $\text{NaCo}_2\text{O}_4$  single crystals. *Phys. Rev. B* 56, R12685.
- [3] Takahata, K., Iguchi, Y., Tanaka, D., Itoh, T., and Terasaki, I. (2000). Low thermal conductivity of the layered oxide  $(\text{Na,Ca})\text{Co}_2\text{O}_4$ : Another example of a phonon glass and an electron crystal. *Phys. Rev. B* 61, 12551.
- [4] Ohtaki, M., Tsubota, T., Eguchi, K., and Arai, H. (1996). Hightemperature thermoelectric properties of  $(\text{Zn}_{1-x}\text{Al}_x)\text{O}$ . *J. Appl. Phys.* 79, 1816.
- [5] Bérardan, D., Guilmeau, E., Maignan, A., and Raveau, B. (2008). Enhancement of the thermoelectric performances of  $\text{In}_2\text{O}_3$  by the coupled substitution of  $\text{M}^{2+}/\text{Sn}^{4+}$  for  $\text{In}^{3+}$ . *J. Appl. Phys.* 104, 064918.
- [6] Okuda, T., Nakanishi, K., Miyasaka, S., and Tokura, Y. (2001). Large thermoelectric response of metallic perovskites:  $\text{Sr}_{1-x}\text{La}_x\text{TiO}_3$  ( $0 < x < 0.1$ ). *Phys. Rev. B* 63, 113104.
- [7] Ohta, S., Nomura, T., Ohta, H., and Koumoto, K. (2005). High-temperature carrier transport and thermoelectric properties of heavily La- or Nb-doped  $\text{SrTiO}_3$  single crystals. *J. Appl. Phys.* 97, 034106.
- [8] Sakai, A., Kannon, T., Takahashi, K., Yamada, Y., Adachi, H. (2010). Large anisotropic thermoelectricity in perovskite related layered structure:  $\text{Sr}_n\text{Nb}_n\text{O}_{3n+2}$ ,  $n = 4, 5$
- [9] Kobayashi, W., Hayashi, Y., Matsushita, M., Yamamoto, Y., Terasaki, I., Nakao, A., Nakao, H., Murakami, Y., Moritomo Y., and Karppinen, M. (2011) Anisotropic thermoelectric properties associated with dimensional crossover in quasi-one-dimensional  $\text{SrNbO}_{3.4+d}$  ( $d \sim 0.03$ ). *Phys. Rev. B* 84, 085118.
- [10] Lee, S., Dursun, S., Duran C., and Randall, C. A. (2011). Thermoelectric power factor enhancement of textured ferroelectric  $\text{Sr}_x\text{Ba}_{1-x}\text{Nb}_2\text{O}_{6-\delta}$  ceramics. *J. Mater. Res.* 26, 26.
- [11] Aguirre, M. H., Logvinovich, D., Bocher, L., Robert, R., Ebbinghaus, S. G., and Weidenkaff, A. (2009). High-temperature thermoelectric properties of  $\text{Sr}_2\text{RuYO}_6$  and  $\text{Sr}_2\text{RuErO}_6$  double perovskites influenced by structure and microstructure. *Acta Mater.* 57, 108.
- [12] Matsuhira K, Sekine C, Paulsen C, Wakeshima M, Hinatsu Y, Kitazawa T, Kiuchi Y, Hiroi Z and Takagi S. (2009). Spin freezing in the pyrochlore antiferromagnet  $\text{Pr}_2\text{Zr}_2\text{O}_7$ . *J. Phys.: Conf. Ser.* 145 012031.

- [13] Kimura, K., Nakatsuji, S., Wen, J-J, Broholm, C., Stone, M. B., Nishibori, E., and Sawa, H. (2013). Quantum fluctuations in spin-ice-like  $\text{Pr}_2\text{Zr}_2\text{O}_7$ . *Nat. Commun.* 4 1934
- [14] Kimura, K., and Nakatsuji, S. (2013). Single-crystal study on the low-temperature magnetism of the pyrochlore magnet  $\text{Pr}_2\text{Zr}_2\text{O}_7$ . *J. Korean Phys. Soc.* 63 719.
- [15] Koteswara Rao K., Banu T., Vithal M., Swamy G. Y. S. K., and Ravi Kumar K. (2002). Preparation and characterization of bulk and nano particles of  $\text{La}_2\text{Zr}_2\text{O}_7$  and  $\text{Nd}_2\text{Zr}_2\text{O}_7$  by sol-gel method *Mater. Lett.* 54 205.
- [16] Lutique S, Javorský P, Konings R J M, van Genderen A C G, van Miltenburg J C and Wastin F. (2003). Low temperature heat capacity of  $\text{Nd}_2\text{Zr}_2\text{O}_7$  pyrochlore. *J. Chem. Thermodynamics* 35 955.
- [17] Zhang F X, Lian J, Becker U, Wang L M, Hu J, Saxena S and Ewing R C. (2007). Structural distortions and phase transformations in  $\text{Sm}_2\text{Zr}_2\text{O}_7$  pyrochlore at high pressures. *Chem. Phys. Lett.* 441 216.
- [18] Singh S, Saha S, Dhar S K, Suryanarayanan R, Sood A K and Revcolevschi A. (2008). Manifestation of geometric frustration on magnetic and thermodynamic properties of the pyrochlores  $\text{Sm}_2\text{X}_2\text{O}_7$  (X= Ti, Zr). *Phys. Rev. B* 77 054408.
- [19] Radha A V, Ushakov S V and Navrotsky A (2009). Thermochemistry of lanthanum zirconate pyrochlore. *J. Mater. Res.* 24 3350
- [20] Kopan A R, Gorbachuk M P, Lakiza S M and Tischchenko Y S. (2010). Low-temperature heat capacity of samarium zirconate ( $\text{Sm}_2\text{Zr}_2\text{O}_7$ ). *Powder Metall. Met. Ceram.* 49 317
- [21] Chiu C-W, Lee Y-H, Sheu H-S and Kao H-C I. (2010). Phase Transition and the Thermal Activated Ordering of the Ions with Pyrochlore Phase in  $\text{Ln}_2\text{Zr}_2\text{O}_7$  (Ln = Sm, Eu) *J. Chinese Chem. Soc.* 57 925
- [22] Blanchard P. E. R., Clements R, Kennedy B J, Ling C D and Reynolds E. (2012). Investigating the order-disorder phase transition in  $\text{Nd}_{2-x}\text{Y}_x\text{Zr}_2\text{O}_7$  via diffraction and spectroscopy. *Inorg. Chem.* 51 13237
- [23] Subramanian M. A., Aravamudan G., and Subba Rao G. V. (1983) "Oxide Pyrochlores—A Review," *Prog. Solid State Chem.*, 15 55–143.
- [24] Quiroz A, Chavira E, Garcia-Vazquez V, Gonzalez G, and Abatal M. (2018). Structural, electrical and magnetic properties of the pyrochlorate.  $\text{Er}_{2-x}\text{Sr}_x\text{Ru}_2\text{O}_7$  ( $0 \leq x \leq 0.10$ ) system. *Revista Mexicana de Física* 64 (3) 222–227.
- [25] Neamen, D.A. (2012). *Semiconductor physics & devices: basic principles*, 4th edn. McGraw-Hill, New York.
- [26] Lu, Y., Nozue, T., Feng, N., Sagara, K., Yoshida, H., Jin, Y. (2015). Fabrication of thermoelectric  $\text{CuAlO}_2$  and performance enhancement by high density. *J. Alloys Compd.* 650:558–563.
- [27] Park. K, Ko, KY, Seo, W. S. (2005) Thermoelectric properties of  $[\text{SEP}]_{\text{CuAlO}_2}$ . *J. Eur. Ceram. Soc.* 25:2219–2222.
- [28] Tate, J., Ju, HL., Moon, J. C., Zakutayev, A., Richard, A. P., Russell,  $[\text{SEP}]_{\text{J}}$ , McIntyre, D. H. (2009). Origin of p-type conduction in single-crystal  $\text{CuAlO}_2$ . *Phys. Rev. B.* 80:165206.